SSRG International Journal of Electronics and Communication Engineering
ISSN: 2348-8549/ https://doi.org/10.14445/23488549/IJECE-V10I12P108

Volume 10 Issue 12, 83-92, December 2023

Original Article

Harnessing EEG Data to Explore Stress Reduction through Hypnosis

Swati Kamthekar[1], Brijesh Iyer[1*], Prachi Deshpande[2], Manjiri Gokhale[3]

[1]*Department of Electronics and Telecommunication, Dr. Babasaheb Ambedkar Technological University, Maharastra, India.*
[2]*Department of Computer Science & Engineering, Shreeyash College of Engineering & Technology, Maharastra, India.*
[3]*Saunvad Centre for Music and Healing, Maharastra, India.*

**Corresponding Author : brijeshiyer@dbatu.ac.in*

Received: 10 October 2023 Revised: 22 November 2023 Accepted: 12 December 2023 Published: 23 December 2023

Abstract *- The rising prevalence of stress in today's fast-paced world has incited individuals to seek complementary and alternative methods, such as yoga, meditation, and hypnosis, to find solace and peacefulness. Allopathic medicines are increasingly being shunned due to their adverse side effects. Hypnotic susceptibility assessment and stress reduction analysis are critical areas of research. To date, the hypnotic susceptibility was measured with a scale. That scale score was used for the supervised classification of the hypnotic susceptibility of the subject using EEG-like inputs. Scale scores are subjective and, hence, may be prone to errors. This paper reports a novel approach that utilizes only EEG-based evaluation of hypnotic susceptibility. The subjects classified with medium and high susceptibility were considered for stress reduction and EEG analysis using hypnosis. For hypnotic susceptibility analysis, Redefined Composite Multiscale Dispersion Entropy (RCMDE) and Multivariate Dispersion Entropy (MvDE), along with an unsupervised K-means classifier, were used. For stress analysis, alpha and beta asymmetry are used as features. The results obtained from this approach deliver valuable insights into hypnotic susceptibility and stress reduction, contributing to the advancement of EEG-based assessment methods.*

Keywords *- Alpha beta asymmetry, Complementary medicine, Entropy, EEG signal, Multivariate, Stress reduction.*

1. Introduction

Stress is a usual response to challenges and demands, and if it persists for a longer duration, it affects individuals positively and negatively. However, conventional stress reduction medicines often carry harmful side effects, which have led to a growing interest in complementary and alternative approaches. Stress detection is reported using features like alpha asymmetry, theta beta ratio, functional connectivity analysis, Heart Rate Variability (HRV) [1, 2] and EEG Fusion. Alpha asymmetry considers asymmetry between the left and right lobes of the brain, and increased right lobe activity indicates stress in the individual. A rise in the theta-to-beta ratio highlights stress-full conditions. During stress, the synchronization between brain lobes reduces, and there is minimal information flow between brain lobes [3, 4].

Generally, stress reduction obtained by allopathic medicine has an adverse effect. Hence, the use of meditation, yoga, and hypnosis as complementary and alternative methods has become a priority [5, 6, 23-25]. Meditation requires practice, and yoga has different poses of body parts that are not possible for people of all age groups and people with spondylitis, knee pain, and similar diseases. Hypnosis is a result-oriented technology for stress reduction. Progressive muscular relaxation is body relaxation; here, every part of the body is relaxed one after the other. Guided imagery, deep breathing and relaxation, and positive affirmations are commonly used hypnosis techniques [7, 8]. Guided imagery is viewed as an effective method as the subject is in a hypnotized state while following instructions, and by imagining vivid mental creations, the mind is gently diverted, and the adoption of relaxation is made possible [9, 10].

Guided hypnosis, unlike methods that impose stringent instructions such as focusing on the breath or specific body parts, offers a more flexible and inclusive approach. This makes it accessible to individuals of all age groups, allowing them to engage in the hypnotic process without the constraints of rigid directives.

Before the application of hypnosis therapy on any person, his or her hypnotic susceptibility should be evaluated; it will add weight to the accuracy of the results. Hypnotic susceptibility can be evaluated using different scales like the Stanford Hypnotic Susceptibility Scale Form C (SHSS-C), Harvard Group Scale of Hypnotic

Susceptibility, Form A (HGSHS:A), Waterloo–Stanford Group Scale (WSGS), the Sussex-Waterloo Scale of Hypnotisability (SWASH), and the Barber Suggestibility Scale (BSS) [11-13]. These scale scores are subjective, so EEG features along with scales are utilized to identify the hypnotic susceptibility of each subject.

Previous work reported EEG features like scaling exponent, phase coherence, fractal dimension, autoregressive coefficients, correlation, and coherence components band power, Higuchi dimension and entropy like EMD entropy, wavelet entropy, and differential entropy are used in combination with hypnotic susceptibility scale [14-17, 24-27] and supervised classification is applied to classify subjects into the low, medium, and highly susceptible people. The classification of labelled data (labelled using scale score) is performed using a supervised learning algorithm like Support Vector Machine (SVM), K-Nearest Neighbour, Fuzzy NN (FNN), and Neural Network (NN) [18].

The reported methods of stress detection are based on either biological, hormonal or skin temperature detection methods. These methods show variable findings for the same set of experiments. Hence, a robust measure is essential, which will be independent of the experimentation method. Further, scale-based labelling for hypnotic susceptibility and stress is prone to error due to the subjectivity involved in it. Hence, a method which reads the real-time brain status of the subject under test to estimate hypnotic susceptibility is the need of the hour.

Hence, the reported work in this paper proposed an EEG-based hypnotic susceptibility detection using unsupervised classifiers for the estimation of stress reduction of medium and highly susceptible subjects.

2. The Methodology

A study was conducted with 30 participants (12 male and 18 female) aged 18 to 60 years. In general, the younger age group tends to experience lower levels of stress. However, beyond the age of 60, there is an increased likelihood of comorbidity arising from health-related issues and diseases.

While incorporating the age group above 60 into stress reduction methods can be beneficial, it is essential to recognize that the stressors may be distinct. Employing varied forms of hypnosis or customized instructions tailored to specific issues can yield more precise results among older adults. This is the rationale behind selecting subjects within the age group of 18 to 60 years for the experimentation detailed in this paper. They were members of the Saunvad Center for Music and Healing Thane-India. They had not participated in any research study before. All were right-handed and healthy. The experiment was performed in a noise-free room during the daytime, particularly from 10 a.m. to 5 p.m. The room was thoughtfully designed for the study, creating a calming atmosphere with dim lighting and comfortable seating arrangements for the participants. Before starting the experiment, participants were given a detailed explanation of the process and asked to sign a written consent form. Permission from the ethical committee was taken for the experiment.

Figure 1 describes the graphical abstract of the proposed system. It consists of tailored audio instructions as input to the human for the experiment. An EEG sensor on the head of a human subject collects the brain wave alterations and transfers the signals to the laptop using EMOTIVE PRO software and Bluetooth module.

This completes the acquisition of EEG signals and stores them for offline processing. Desired features are extracted from the EEG signal, and then the classifier classifies the signals into low, medium and high susceptibilities. The high and medium susceptibility signals are further used for stress detection.

The work reported in this paper is divided into two parts. The hypnosis susceptibility is initially evaluated, and then stress analysis is carried out using it. The hypnosis susceptibility is estimated using redefined complex multiscale and multivariate dispersion entropy. Limitations of the extensively used and potent Multiscale Entropy (MSE) have the potential for undefined MSE values in small signals and the sluggish presentation of MSE in real-time applications.

Hence, after careful comparison, the entropies with the fastest speed and the lowest computational complexity for long signals is selected for the calculation of features for hypnosis-level detection. Each entropy was considered individually, and K-means classifiers were used to classify the subjects into low, medium, and high susceptibilities. The stress detection is computed with alpha-beta asymmetry. Here, the mean spectral density of each time series was calculated by taking a ratio of right brain to left brain activation, and then stress reduction was concluded.

2.1. Multivariate Dispersion Entropy

Multivariate Dispersion Entropy (MvDE) is an advanced variation of the univariate Dispersion Entropy (DisEn) technique. It allows for assessing DisEn from multiple input time series, making it suitable for analyzing complex data. Like its univariate counterpart, each time series is pre-processed using a mapping function, resulting in a multivariate set of S-input time series. This process allows a complete estimation of entropy across multiple dimensions, enhancing the understanding and analysis of complex systems.

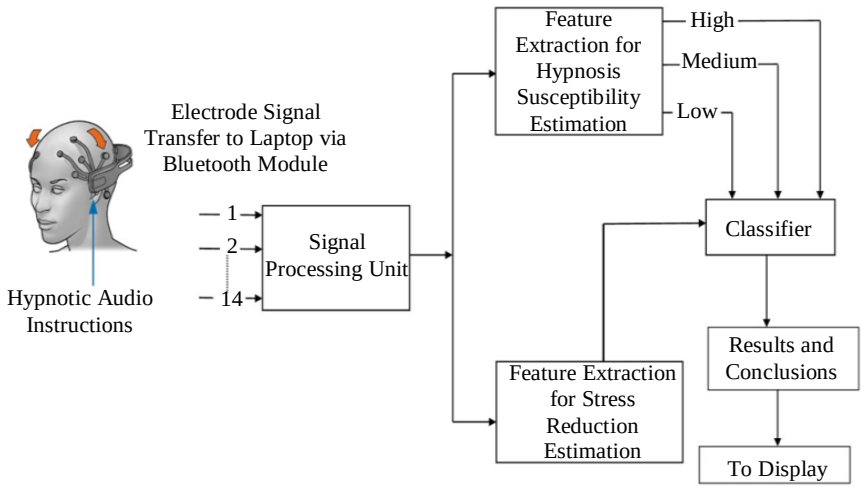

Fig. 1 Graphical abstract of the proposed method

$$P = \{p_{k,i}\}_{k=1,2,....S}^{i=1,2,....N} \quad (1)$$

N is the length of the time series. The steps to calculate MvDE are:

2.1.1. Step 1: Creation of Univariate Quantized Time-Series

Step 1 design of univariate quantized time-series - The amplitude values of each time series are spread into a predetermined number of classes (c) individually. The signal samples of each participant are allotted to the appropriate class based on their amplitudes. This process generates a quantized time series (*uj*, where *j = 1, 2, 3, ..., N*) for each input time series, resulting in a set of S quantized time series.

$$U = \{u_{k,i}\}_{k=1,2,3...S}^{i=1,2,3....N} \quad (2)$$

2.1.2. Step 2: Construction of Multivariate Embedded Vectors

An embedding dimension (m) and time delay (d) are chosen to create multivariate embedded vectors. This process generates univariate embedded vectors of length m from each signal, following a similar approach to univariate DisEn. The resulting univariate embedded vectors are then organized into p-synchronized vectors containing one vector from each input signal. Within each set, the vectors are concatenated to form corresponding multivariate embedded vectors *(Z(j))* of length mp, where j ranges from 1 to *N - (m-1) d.*

2.1.3. Step 3: Mapping to Multiple Dispersion Patterns

In MvDE, each embedded vector is associated with multiple dispersion patterns. Every subset of m elements in *Z(j)* is analyzed, considering all probable $\binom{mp}{m}$ combinations. This formulates $\phi_q(j)(q = 1,2, \ldots \binom{mp}{m}$ subsectors are then matched to their corresponding $\pi_{v_0.....v_{m-1}}$ dispersion patterns.

Correspondingly, the entire number of dispersion pattern instances is$(N-(M-1)d)\binom{mp}{m}$and the number of unique dispersion patterns is *Cm.*

2.1.4. Step 4: Computation of Dispersion Pattern Relative Frequency

The relative frequency of each dispersion pattern is computed using a similar approach as Equation (1), with necessary adjustments made to accommodate the more significant number of instances:

$$p\left(\pi_{v_0.....rv_{m-1}}\right) = \frac{\left(\#\left\{\substack{j \\ j \le N-(m-1)d, \emptyset_q(j) has\ type\ \pi_{v_0.....v_{m-1}}}\right\}\right)}{(N-(m-1)d)\binom{mp}{m}} \quad (3)$$

2.1.5. Step 5: Estimation of Multivariate Dispersion Entropy

The collected relative frequencies estimate the corresponding multivariate DisEn value based on Shannon's entropy definition:

$$mvDE(X,m,c,d) = -\sum_{\pi=1}^{c^m} p\left(\pi_{v_0.....=v_{m-1}}\right) \ln\left(p\left(\pi_{v_0.....-v_{m-1}}\right)\right) \quad (4)$$

As described in the steps above, the algorithmic distinction employed in this study lies in the fourth step, which introduces variations to the MvDE algorithm as suggested by its creators.

2.2. Redefine Composite Multiscale Dispersion Entropy

In Randomized Coarse Multiscale Dispersion Entropy (RCMDE), τ multiple time series are generated by considering different starting points to the coarse-graining procedure. The RCMDE feature value is then determined by calculating the Shannon entropy of the mean dispersion patterns of these shifted sequences. The k^{th} course grained time.

$X_k^{(\tau)} = \{x_{k.1}{}^{\tau}\ x_{k.2}{}^{\tau} \dots \dots .\}$ of u is as follows,

$$x_{kj}^{\tau} = \frac{1}{T}\sum_{b=k+\tau(j-1)}^{k+\tau j-1} u_b\,,\ \ 1 \le j \le N\,, 1 \le k \le \tau \quad (5)$$

Then, for every scale factor, RCMDE is defined as follows:

$$RCMED(X,m,c,d,\tau) = -\sum_{\pi=1}^{c^m} \bar{p}\left(\pi_{v_0 \dots\dots = v_{m-1}}\right) \ln\left(\bar{p}\left(\pi_{v_0 \dots\dots - v_{m-1}}\right)\right) \quad (6)$$

2.3. K-Means Classifier

K-means classifier is selected to classify the EEG signals as it is computationally efficient and can handle large data sets. It is straightforward to comprehend and apply, requiring only a minimal number of features and steps. Furthermore, it is swift and scalable, capable of efficiently managing extensive datasets through parallelization or distribution [23]. K-means is a centroid-based approach that identifies the items that will make up the clusters using a particular cluster's centroid (ci). Distance-based clustering strategies are used. The Euclidean distance, the square root of the differences between two positions, is used to calculate the distance.

$$Euclidian\ Distance(D1) = \sqrt[2]{\sum_{i=1}^{k}\left(x_{ik} - x_{jk}\right)^2} \quad (7)$$

The k initial clusters are used to divide the n total observations into subsets, and by calculating the distance (disp (x, ci)), the differences between items (x) and clusters (ci) that fit into a cluster are determined. The total squared error of all the objects in a cluster is used to find the cluster variation (Ci).

The new cluster centre is determined by computing the mean of all data points within the cluster, utilizing the following equation:

$$\mathrm{v} = \frac{1}{\mathrm{c_i}}\sum_{1}^{\mathrm{c_i}} \mathrm{x_i}. \quad (8)$$

2.4. Alpha-Beta Asymmetry

Alpha-beta asymmetry is a measure used to assess the variation in excitation levels among homogeneous electrodes during cognitive tasks or activities. Numerous studies have explored alpha asymmetry's application in identifying stress reduction strategies. The investigation reported in [26] specifically focused on the impact of binaural beats on EEG alpha asymmetry in individuals experiencing stress.

The results showed a significant reduction in alpha asymmetry as well as a notable shift towards increased relative activation in the left hemisphere. Long-term stress is evaluated using alpha and beta asymmetry with four channels, along with EEG analysis [20]. PSS scale and expert evaluation are also considered to label the data. Expert evaluation-based labelled data gives 82 % accuracy with the SVM classifier [19]. Workplace noise creates stress, and that was estimated using frontal alpha asymmetry [21]. Only four electrodes-f_3, f_4, f_7, f_8 were analyzed. Here, electrodes f_3 and f_4 showed a greater activation due to a noisy environment.

Beta waves are also used as a measure of high-frequency variations due to stress. The reported studies used different stress scales, questionnaires, pathological tests, or expert evaluations to label EEG data. In the present study, no scale, questionnaire, or pathological test is used to label the data. An unsupervised k-means classifier classifies data.

Our study is focused on the alpha and beta frequency bands, which were further classified into lower and higher beta bands. The degree of asymmetry was calculated as the ratio of the difference between the left and right homogenous electrodes' excitation levels and divided by the sum of their excitations to determine the degree of asymmetry. This method allowed us to measure asymmetry in both the frontal and temporal lobes, widely recognized as a reliable indicator of stress. This is because stress, a negative emotion, naturally induces increased excitation in the right hemisphere.

During our analysis, power spectral density estimations were used for four time series (f_3, f_4, t_7, *and* t_8) across three different frequency bands: alpha, lower beta, and higher beta. These estimations were carried out distinctly for the temporal and frontal lobes. The alpha-beta asymmetry ratio was evaluated using Equations 9 to 14.

$$\alpha f = \frac{(\alpha AF_4 - \alpha AF_3)}{(\alpha AF_4 + \alpha AF_3)} \quad (9)$$

$$\alpha t = \frac{(\alpha t_8 - \alpha t_7)}{(\alpha t_8 + \alpha t_7)} \quad (10)$$

$$\beta\ lf = \frac{(\beta lAF_4 - \beta lAF_3)}{(\beta lAF_4 + \beta lAF_3)} \quad (11)$$

$$\beta\ lt = \frac{(\beta lt_8 - \beta lt_7)}{(\beta lt_8 + \beta lt_7)} \quad (12)$$

$$\beta\ hf = \frac{(\beta hAF_4 - \beta hAF_3)}{(\beta hAF_4 + \beta hAF_3)} \quad (13)$$

$$\beta\ ht = \frac{(\beta ht_8 - \beta ht_7)}{(\beta ht_8 + \beta ht_7)} \quad (14)$$

3. Results and Discussion

Earlier investigations have utilized scale scores to determine patients' susceptibility to hypnosis and gauge their pre and post-intervention stress levels using perceived stress scales. However, these scores were subjective and susceptible to errors associated with assigned tasks and

expert opinions. Consequently, supervised categorization based on these scores yielded less precise outcomes. To address this limitation, this study proposes an alternative approach by leveraging EEG-based analysis for hypnosis detection. In the present work, specifically, we employ Redefined Composite Multiscale Dispersion Entropy (RCMDE) and Multivariate Dispersion Entropy (MvDE) in combination with an unsupervised K-means classifier applied for hypnosis-level detection. This innovative methodology offers a more unbiased and reliable means of assessing hypnotic susceptibility, overcoming the limitations associated with subjective scale scores and task-dependent evaluations.

After classifying the subjects, stress reduction in individuals was examined with high and medium hypnotic susceptibility. In particular, alpha asymmetry and beta asymmetry in the frontal and temporal regions of the brain were analyzed by paying particular attention to differentiating between low and high beta waves. Our stress analysis using imagery hypnosis only included subjects with high or medium susceptibility, as judged by their entropy scores. The outcome of the K-means classifier is depicted in Figure 2, categorizing 57% and 53% of individuals as having medium and high susceptibility, respectively, based on RCMDE and MvDE. Subsequently, these identified individuals underwent an assessment of alpha-beta asymmetry in the frontal and temporal lobes for stress analysis. Figures 3 and 4 illustrate the fluctuations in the average measurements for 16 and 17 participants who were evaluated as having medium and high susceptibility, respectively, utilizing the two entropy measures. Table 1 provides the results of alpha-beta asymmetry measurements of the subjects is shown in Appendix.

Figure 3 exhibits the results of the MvDE-based classification, which illustrates the average variations in alpha and beta spectral density across all 16 participants, providing insights into the asymmetry between the left and right hemispheres.

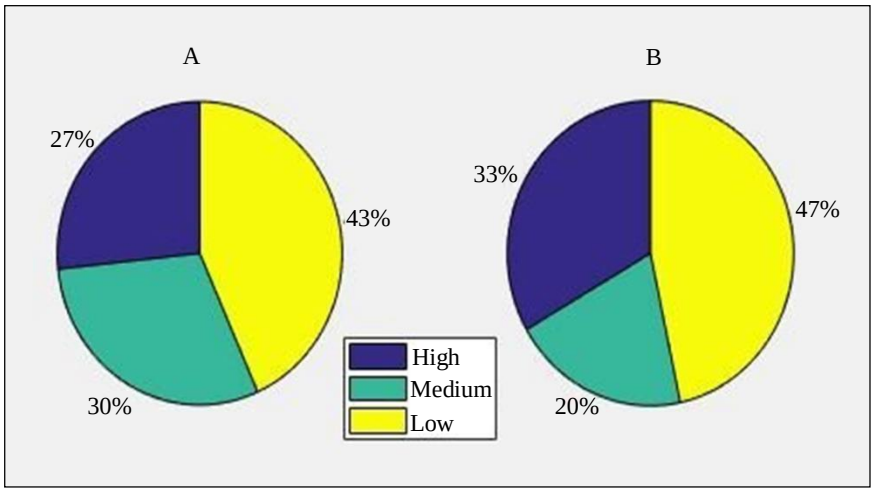

Fig. 2 Classification result of hypnosis level detection: a) RCMDE, and b) MVDE.

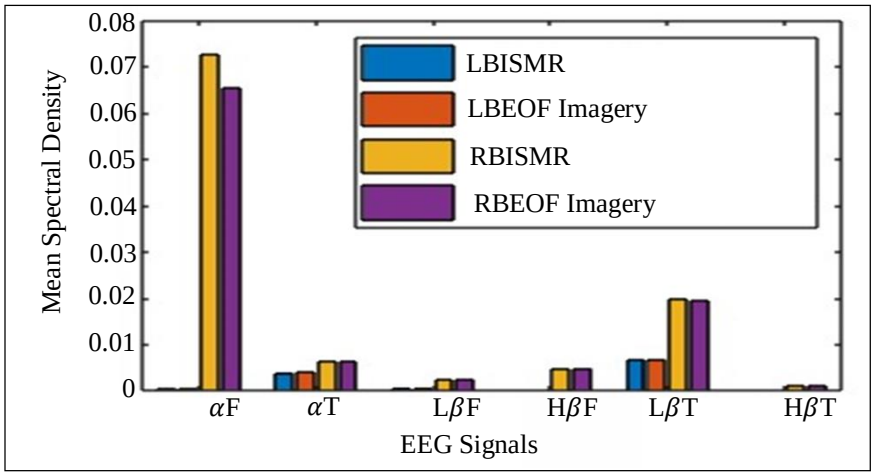

Fig. 3 Average of 16 participants hypnotically susceptible using MVDE

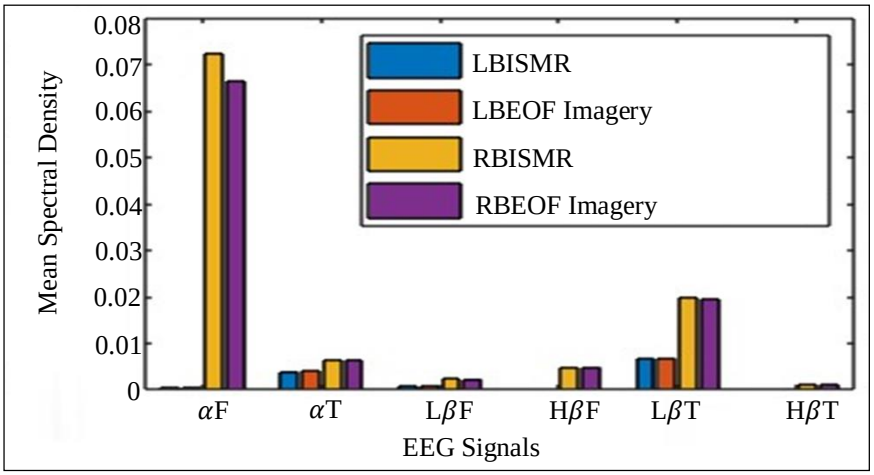

Fig. 4 Average calculation of 17 participants with hypnotic susceptibility using RCMDE

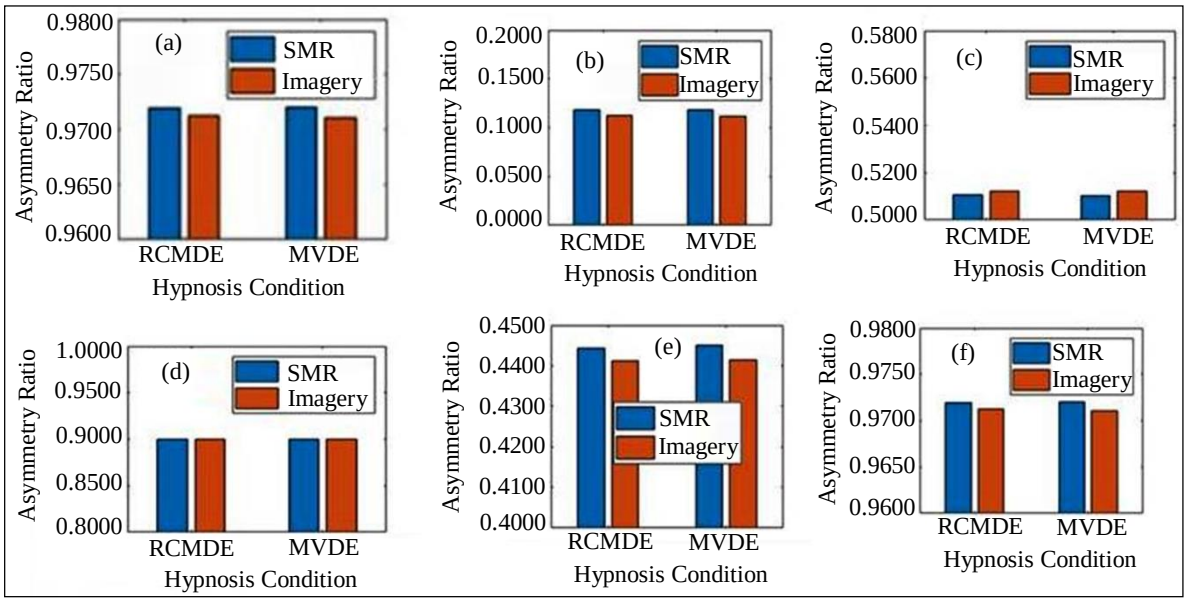

Fig. 5 Variation of asymmetry ratio in frontal and temporal lobes using both entropies: (a) Alpha frontal ratio, (b) Alpha temporal ratio, (c) Beta L frontal ratio, (d) Beta H frontal ratio, (e) Beta L temporal ratio, and (f) Beta H temporal ratio.

The graph demonstrates that the mean spectral density values for SMR were either equal to or higher than those of the imagery signal. It is observed that significant variation of spectral density is observed in the alpha band in frontal and lower beta temporal lobe values. The imagery signal values showed a decrease compared to the initial SMR values.

Additionally, the graph demonstrates that the values in the left hemisphere were significantly lower than those in the right lobe. Upon closer examination, we found that left lobe variations were enhanced, showing variations in the alpha and beta temporal regions. On the other hand, variations in the right hemisphere were observed in the alpha-frontal and lower beta-frontal regions. The results obtained from RCMDE are shown in Figure 4. It shows the overall average variations, left lobe variations, and right lobe variations, respectively. It demonstrates a significant decrease in the imagery signal at alpha frontal and lower beta temporal locations. Our analysis primarily focused on the right hemisphere, specifically the Mean Spectral Density (MSD), during the initial samples of SMR and the last few samples of imagery hypnosis across all participants in the imagery hypnosis analysis.

Figure 5 visually represents the dynamics of average alpha and beta asymmetrical ratios. These ratios measure the asymmetry between the left and right brain lobes, computed using Equations 9 to 14. The figure provides insights into the variations observed in these ratios throughout the study. A larger ratio indicates a significant difference, with higher values on the right side. According to the results for A, B, D, and E, the ratio value during imagery was lower, suggesting that the right-side values were notably lower during the imagery session than in the SMR condition.

Table 2. Qualitative comparative analysis of stress detection methods

References	Stress Markers	No. of Electrodes	Scale	Cost Functions Used
[20]	Alpha-Beta Asymmetry	4	PSS, Expert Evaluation	--
[22]	Frontal Alpha Asymmetry	4 (f_3,f_4,f_7,f_8)	Salivary-Alpha Amylase (SAA)	--
[27]	Alpha Asymmetry	4	DASS	--
Proposed Method	**Alpha-Beta Asymmetry**	**4**	**Scale Independent; EEG Data is Used with Hypnosis**	**RCMDE and MVDE**

This reduction further confirms the decrease in stress. Notably, the plots consistently demonstrate a notable decrease in magnitude in the alpha band of the frontal lobe and the lower beta band of the temporal lobe.

Table 2 provides a qualitative comparative analysis of the proposed method. Present day stress detection methods utilize physiological changes, hormones, and skin temperature as stress identifiers. However, the findings with these stressors are not proven to be consistent. The reason is that these changes may not always be due to stress. Further, different scales are used to decide the stress score [21, 27]. This is a subjective method to evaluate stress before and after the intervention. The salivary tests predefine scale scores, which are also used to label the data set and to evaluate the accuracy of the result of the EEG evaluation of stress. However, in the reported methods in this paper, EEG data is used for the analysis of stress reduction.

EEG is an exact impression of emotions or brain activities. Hence, a more authentic and bias-free evaluation can be achieved using the reported method. Hence, the reported method in this paper is scale-independent and, in turn, is free from subjectivity in the analysis stress. Further, a high degree of cooperation is required with a scale-based method as more sittings may be required to predict the outcomes. However, the reported method collects the data in only one hypnosis sitting. The study indicates that guided imagery hypnosis is a practical approach to reducing stress.

Significant improvement in the reduction of stress is observed in a single session of imagery hypnosis, validating alpha beta asymmetry as a stress marker. Consequently, stress induction techniques were not used. If these techniques had been employed, a significant disparity was observed between the initial and the final SMR samples during the imagery hypnosis session.

It is reasonable to expect that the stress reduction effects would become even more prominent with regular hypnosis practice over a more extended period. Stress reduction through alternative methods offers distinct advantages as it is safe and poses no adverse effects on individuals. This non-invasive approach ensures zero risk to the subject's life.

Hypnosis, being devoid of harmful consequences, is suitable for individuals across all age groups. The EEG signal, being impervious to manipulation, provides direct insights from the brain, offering an accurate reflection of emotions, sensitivity, and thoughts.

The purely EEG-based detection of hypnosis levels furnishes valuable information about the subject's response to the hypnotic process. By focusing exclusively on medium and high hypnotic susceptibility subjects, the effectiveness of hypnosis is more precisely gauged. This method proves to be both accurate and highly efficient, often yielding significant stress reduction benefits in just one session. However, when dealing with elderly subjects aged 60 and above, tailored instruction sets may be necessary, taking into account their specific comorbidities for optimal results.

4. Conclusions

The K-means classifier effectively categorized participants, facilitating the selection of individuals with medium and high susceptibility for stress reduction through guided imagery hypnosis. A notable reduction in stress was observed after a single session of imagery hypnosis, affirming the validity of alpha-beta asymmetry as a reliable stress marker.

Specific participants exhibited a substantial decrease, up to 34%, in both alpha-temporal and lower beta-temporal parameters. The incorporation of features from RCMDE and MVDE, along with a solely EEG-based approach, significantly enhances the accuracy of this stress reduction method.

EEG, being a direct reflection of emotional states, renders the proposed approach a more genuine and impartial evaluation. In comparison to other stress assessment approaches, the proposed method stands out, offering a complementary and distinctive perspective on stress evaluation.

Ethical Statement

The work reported in this paper has received approval from the University's ethical committee.

References

[1] Jyoti Sekhar Banerjee, Mufti Mahmud, and David Brown, "Heart Rate Variability-Based Mental Stress Detection: An Explainable Machine Learning Approach," *SN Computer Science*, vol. 4, 2023. [CrossRef] [Google Scholar] [Publisher Link]

[2] M. Ben Ayed, "Balanced Communication-Avoiding Support Vector Machine when Detecting Epilepsy Based on EEG Signals," *Engineering, Technology and Applied Science Research*, vol. 10, no. 6, pp. 6462-6468, 2020. [CrossRef] [Google Scholar] [Publisher Link]

[3] Tee Yi Wen, and Siti Armiza Mohd Aris, "Electroencephalogram (EEG) Stress Analysis on Alpha/Beta Ratio and Theta/Beta Ratio," *Indonesian Journal of Electrical Engineering and Computer Science*, vol. 17, no. 1, pp. 175-182, 2020. [CrossRef] [Google Scholar] [Publisher Link]

[4] Ala Hag et al., "EEG Mental Stress Assessment Using Hybrid Multi-Domain Feature Sets of Functional Connectivity Network and Time-Frequency Features," *Sensors*, vol. 21, no. 18, pp. 1-23, 2021. [CrossRef] [Google Scholar] [Publisher Link]

[5] Helané Wahbeh et al., "Complementary and Alternative Medicine for Posttraumatic Stress Disorder Symptoms: A Systematic Review," *Journal of Evidence-Based Integrative Medicine*, vol. 19, no. 3, pp. 161-175, 2014. [CrossRef] [Google Scholar] [Publisher Link]

[6] Pallav Sengupta, "Health Impacts of Yoga and Pranayama: A State-of-the-Art Review," *International Journal of Preventive Medicines*, vol. 3, no. 7, pp. 444-458, 2012. [Google Scholar] [Publisher Link]

[7] Theodore X. Barber, and Wilfried de Moor, "A Theory of Hypnotic Induction Procedures," *American Journal of Clinical Hypnosis*, vol. 15, no. 2, pp. 112-135, 1972. [CrossRef] [Google Scholar] [Publisher Link]

[8] Loren Toussaint et al., "Effectiveness of Progressive Muscle Relaxation, Deep Breathing, and Guided Imagery in Promoting Psychological and Physiological States of Relaxation," *Evidence-Based Complementary and Alternative Medicine*, vol. 2021, pp. 1-8, 2021. [CrossRef] [Google Scholar] [Publisher Link]

[9] N. Zech et al., "Efficacy, Acceptability and Safety of Guided Imagery/Hypnosis in Fibromyalgia - A Systematic Review and Meta-Analysis of Randomized Controlled Trials," *European Journal of Pain*, vol. 21 no. 2, pp. 217-227, 2016. [CrossRef] [Google Scholar] [Publisher Link]

[10] Maria Hadjibalassi et al., "The Effect of Guided Imagery on Physiological and Psychological Outcomes of Adult ICU Patients: A Systematic Literature Review and Methodological Implications," *Australian Critical Care*, vol. 31, no. 2, pp. 73-86, 2018. [CrossRef] [Google Scholar] [Publisher Link]

[11] P. Lush et al., "The Sussex-Waterloo Scale of Hypnotizability (SWASH): Measuring Capacity for Altering Conscious Experience," *Neuroscience of Consciousness*, vol. 2021, no. 1, pp. 1-7, 2021. [CrossRef] [Google Scholar] [Publisher Link]

[12] John C. Ruch, Arlene H. Morgan, and Ernest R. Hilgard, "Measuring Hypnotic Responsiveness: A Comparison of the Barber Suggestibility Scale and the Stanford Hypnotic Susceptibility Scale, Form A," *International Journal of Clinical and Experimental Hypnosis*, vol. 22, no. 4, pp. 365-376, 1974. [CrossRef] [Google Scholar] [Publisher Link]

[13] Golnaz Baghdadi, and Ali Motie Nasrabadi, "Comparison of Different EEG Features in the Estimation of Hypnosis Susceptibility Level," *Computers in Biology and Medicines*, vol. 42, no. 5, pp. 590-597, 2012. [CrossRef] [Google Scholar] [Publisher Link]

[14] N.V. Kimmatkar, and B. Vijaya Babu, "Human Emotion Detection with Electroencephalography Signals and Accuracy Analysis Using Feature Fusion Techniques and a Multimodal Approach for Multiclass Classification," *Engineering, Technology & Applied Science Research*, vol. 12, no. 4, pp. 9012-9017, 2022. [CrossRef] [Google Scholar] [Publisher Link]

[15] Elahe' Yargholi, and Ali Motie Nasrabadi, "The Impacts of Hypnotic Susceptibility on Chaotic Dynamics of EEG Signals during Standard Tasks of Waterloo-Stanford Group Scale," *Journal of Medical Engineering & Technology*, vol. 37, no. 4, pp. 273-281, 2013. [CrossRef] [Google Scholar] [Publisher Link]

[16] Riccardo Chiarucci et al., "Cross-Evidence for Hypnotic Susceptibility through Nonlinear Measures on EEGs of Non-Hypnotized Subjects," *Scientific Reports*, vol. 4, no. 1, 2014. [CrossRef] [Google Scholar] [Publisher Link]

[17] Graham A. Jamieson, and Adrian P. Burgess, "Hypnotic Induction is Followed by State-Like Changes in the Organization of EEG Functional Connectivity in the Theta and Beta Frequency Bands in High-Hypnotically Susceptible Individuals," *Frontiers in Human Neuroscience*, vol. 8, pp. 1-11, 2014. [CrossRef] [Google Scholar] [Publisher Link]

[18] P.N. Smyrlis, D.C. Tsouros, and M.G. Tsipouras, "Constrained K-Means Classification," *Engineering, Technology & Applied Science Research*, vol. 8, no. 4, pp. 3203-3208, 2018. [CrossRef] [Google Scholar] [Publisher Link]

[19] Emad Alyan, Naufal M. Saad, and Nidal Kamel, "Effects of Workstation Type on Mental Stress: FNIRS Study," *Human Factors: The Journal of the Human Factors and Ergonomics Society*, vol. 63, no. 7, pp. 1230-1255, 2021. [CrossRef] [Google Scholar] [Publisher Link]

[20] Sanay Muhammad Umar Saeed et al., "EEG Based Classification of Long-Term Stress Using Psychological Labeling," *Sensors*, vol. 20, no. 7, pp. 1-15, 2020. [CrossRef] [Google Scholar] [Publisher Link]

[21] Emad Alyan et al., "Frontal Electroencephalogram Alpha Asymmetry during Mental Stress Related to Workplace Noise," *Sensors*, vol. 21, no. 6, pp. 1-12, 2021. [CrossRef] [Google Scholar] [Publisher Link]

[22] Jan Moritz Fischer et al., "Stress Reduction by Yoga Versus Mindfulness Training in Adults Suffering from Distress: A Three-Armed Randomized Controlled Trial Including Qualitative Interviews (RELAX Study)," *Journal of Clinical Medicine*, vol. 11, no. 19, pp. 1-23, 2022. [CrossRef] [Google Scholar] [Publisher Link]

[23] Marco Capó, Aritz Pérez, and Jose A. Lozano, "An Efficient K-Means Clustering Algorithm for Tall Data," *Data Mining and Knowledge Discovery*, vol. 34, no. 3, pp. 776-811, 2020. [CrossRef] [Google Scholar] [Publisher Link]

[24] Mehlika Saraç, *A Literature Review on Mindfulness at Work Places: Conceptualization, Measurement, and Outcomes*, Handbook of Research on Positive Organizational Behavior for Improved Workplace Performance, IGI Global, pp. 55-71, 2020. [CrossRef] [Google Scholar] [Publisher Link]

[25] Asma Baghdadi, Yassine Aribi, and Adel M. Alimi, "Efficient Human Stress Detection System Based on Frontal Alpha Asymmetry," *International Conference on Neural Information Processing*: *Neural Information Processing*, pp. 858-867, 2017. [CrossRef] [Google Scholar] [Publisher Link]

[26] Maryam Alimardani et al., "Classification of EEG Signals for a Hypnotrack BCI System," *2018 IEEE/RSJ International Conference on Intelligent Robots and Systems (IROS)*, Madrid, Spain, pp. 240-245, 2018. [CrossRef] [Google Scholar] [Publisher Link]

[27] H. Norhazman et al., "Behaviour of EEG Alpha Asymmetry when Stress is Induced and Binaural Beat is Applied," *2012 International Symposium on Computer Applications and Industrial Electronics (ISCAIE)*, Kota Kinabalu, Malaysia, pp. 297-301, 2012. [CrossRef] [Google Scholar] [Publisher Link]

Appendix

Table 1. Results of alpha-beta asymmetry measurements of the subjects

S.No.	Alpha frontal		Alpha temporal		Beta L Frontal		Beta H Frontal		Beta L temporal		Beta H temporal	
	SMR	Imagery	SMR	Imagery	SMR	Imagery	SMR	Imagery	SMR	Imagery	SMR	Imagery
2	0.983848	0.981332	0.226907	0.228908	0.51534	0.520435	0.999466	0.99946	0.48922	0.489917	0.600746	0.591719
5	0.983845	0.980979	0.348807	0.218016	0.536613	0.52315	0.999468	0.999471	0.488388	0.4671	0.591605	0.588652
8	0.984078	0.98134	0.227934	0.218405	0.524979	0.532917	0.999467	0.999467	0.488849	0.468308	0.584873	0.590973
12	0.98397	0.981345	0.226557	0.230991	0.528668	0.530254	0.999467	0.999468	0.488649	0.488389	0.589687	0.590528
16	0.983901	0.981291	0.230754	0.229484	0.52636	0.522024	0.999467	0.999457	0.488614	0.467463	0.588275	0.589089
18	0.983874	0.98211	0.226922	0.231056	0.530004	0.530337	0.999468	0.999468	0.488077	0.487863	0.589726	0.592799
19	0.98395	0.983033	0.230994	0.229164	0.524209	0.523563	0.999465	0.999465	0.488286	0.48847	0.590979	0.589964
20	0.983995	0.983962	0.23303	0.229164	0.525138	0.523563	0.999467	0.999465	0.489176	0.48847	0.592357	0.589964
22	0.983939	0.981336	0.229379	0.231956	0.524655	0.527331	0.999466	0.99944	0.48748	0.488933	0.592166	0.594989
23	0.983968	0.983012	0.227147	0.227455	0.527676	0.525	0.999466	0.999454	0.488309	0.48904	0.589607	0.588322
24	0.983908	0.983917	0.228806	0.228538	0.529715	0.529891	0.999468	0.999468	0.488313	0.468136	0.590337	0.59069
25	0.983919	0.983927	0.227798	0.22622	0.648692	0.529198	0.999468	0.999469	0.488459	0.488785	0.589153	0.590525
26	0.98395	0.982988	0.22816	0.229008	0.527847	0.529078	0.999466	0.999466	0.4892	0.488605	0.589264	0.588899
27	0.983953	0.983941	0.23683	0.228721	0.526154	0.52497	0.999465	0.999468	0.488425	0.46791	0.590404	0.591449
28	0.984006	0.981367	0.227685	0.234726	0.52498	0.527903	0.999465	0.999465	0.488364	0.489266	0.589733	0.588602
29	0.984054	0.981501	0.223781	0.17193	0.525455	0.530474	0.999467	0.99947	0.488133	0.48699	0.591429	0.590282
30	0.983901	0.983879	0.230754	0.221751	0.52636	0.530769	0.999467	0.999467	0.488614	0.488196	0.588275	0.591326